Proceedings 10th NUMGE 2023
10th European Conference on Numerical Methods in Geotechnical Engineering
Zdravkovic L, Kontoe S, Taborda DMG, Tsiampousi A (eds)

https://doi.org/10.53243/NUMGE2023-369

Effect of strain softening on the prediction of post-failure runout in sensitive clay landslide

Z.A. Urmi[1] , A. Saeidi[1] , A. Yerro[2] , R.V.P Chavali[1]

[1]*Department of Applied Science, Université du Québec à Chicoutimi, Québec, Canada*
[2] *Department of Geotechnical Engineering – Virginia Tech, Blacksburg, Virginia, USA*

ABSTRACT: Due to extensive post-peak strain softening and subsequent remolding of sensitive clays, landslides in these soils result in catastrophic progressive or retrogressive failures. Analysis and prediction of failure initiation and runout of sensitive clay landslides are crucial to reducing their impact; however, the post-failure behavior of such landslides is very complex. The use of advanced numerical techniques capable of accounting for large deformations and the strain-softening of the material is vital to accurately predicting post-failure movements. This study uses the material point method (MPM) to evaluate the influence of strain-softening behavior on the post-failure mechanism and runout of sensitive clay landslides. The simulation has been performed using Anura3D software with a strain-softening Mohr-Coulomb constitutive soil model. In particular, parametric studies are performed on the controlling parameters of the strength-degradation equation to assess strain-softening effects on retrogression and runout distances. The results showed that an increased rate of softening increases post-failure movement. For a fixed peak and remolded shear strength, there is a limiting value of strain-softening factor below which retrogressive failure does not occur.

Keywords: Sensitive clay; strain-softening; retrogressive failure; large-deformation; MPM.

1 INTRODUCTION

Large retrogressive landslides in sensitive clays frequently occur in Scandinavia and eastern Canada. Extensive post-peak strength reduction (Figure 1), generally referred to as "strain softening" in these soils, is considered to be the primary reason for such large-scale landslide occurrences (Locat et al. 2011).

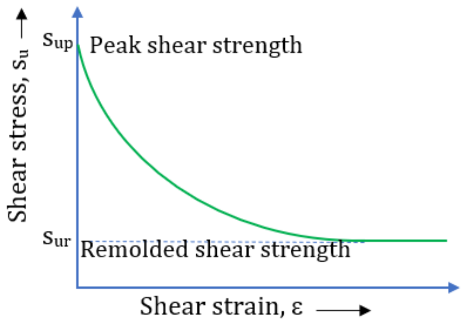

Figure 1. Strain-softening in sensitive clays

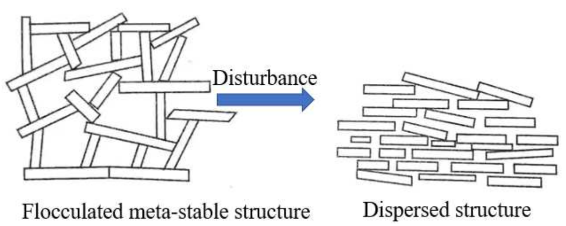

Figure 2. Structural susceptibility of sensitive clays to disturbance

The strain-softening nature of sensitive clays of eastern Canada can be better understood from their depositional features. These soils were deposited in the marine environment on the depressions left by the Laurentian ice sheet around 14000 to 6000 years ago (Lefebvre 1996). Due to the salt ions exposure, the clays formed a flocculated structure with high undisturbed shear strength. After the iso-static rebound, the clays rose above the seawater, and the salt ions leached into the fresh water. As a result, the clay formed a meta-stable structure highly susceptible to disturbance (Figure 2), eventually leading to a substantial loss of shear strength at large strains (Lefebvre 1996). Sensitive clays are thus named after their sensitivity towards the disturbance, and the term sensitivity (S_t) is quantified as the ratio of the peak shear strength (s_{up}) to the reduced (remolded) shear strength (s_{ur}) (Skempton and Northey 1952). When slopes containing sensitive clay layers are subjected to stresses beyond their peak shear strength, strain is localized in the weak soil layers forming narrow shear bands where strength reduces nearly to zero. Failure surfaces are formed along the shear bands, and soil within them loses its intact structure and transforms into a liquid-like mass (remolded soil) that flows (Rosenqvist 1953). These liquified soils either laterally spread or drift away from their original location, resulting in a series of failures proceeding rapidly in a progressive or retrogressive manner (Locat et al. 2011) and eventually destroying areas far away from the site of the initial failure. Thus, the extent of the failure of sensitive clay landslides is enormous, with devastating aftermath compared to slope failure in non-sensitive soil (Figure 3).

Figure 3. Retrogressive landslide in the sensitive clays of Gjerdrum in Eastern Norway on December 30, 2020 (Photo: Anders Martinsen)

The landslide mechanism in a retrogressive failure in sensitive soil involves several complex features such as the landslide trigger, formation of shear bands or multiple failure surfaces, movement of the remolded soil, progression of the landslide, etc. These issues make the numerical analysis of sensitive clay landslides exceptionally challenging. The conventional methods like limit equilibrium or finite element strength reduction used in slope stability analyses suffer from two problems that make them unsuitable for application in sensitive clay slopes. Firstly, these approaches can barely predict the landslide initiation, let alone estimate the subsequent failures or runouts resulting in retrogressive landslides. Secondly, these landslides involve large deformations, which result in mesh tangling in conventional FEM techniques. The strain-softening behavior of sensitive clays responsible for the complex failure mechanism requires a sophisticated constitutive soil model and an advanced numerical tool to handle large deformation problems.

In the last two decades, significant development has been made in the numerical tools to accommodate large deformation problems in geotechnical engineering. Several mesh-based and meshless numerical frameworks like arbitrary lagrangian finite element method, particle finite element method, material point method, etc., have successfully been implemented to model some key characteristics of large retrogressive failures (Wang et al. 2022, Zhang et al. 2018, Tran and Solowski 2019). In this study, the material point method (MPM) is the preferred method for modeling landslide problems. MPM has previously been used to demonstrate the formation of shear bands in retrogressive and sensitive clay spread failure (Wang et al. 2016, Tran and Solowski 2019). The MPM uses a combined Eulerian and Lagrangian framework where particles are described with a collection of Lagrangian material points and governing equations are solved at the computational nodes of a fixed Eulerian background mesh (Sulsky et al. 1994). The movement of material points is free but confined within the background mesh. There are several reasons for choosing MPM; firstly, this method is based on a continuum description of material flow using an Eulerian-Lagrangian approach which makes it well suited for large deformation failure analyses; secondly, the governing equations of MPM and FEM are generally the same which makes its implementation easier for the FEM users; thirdly, Lagrangian description of soil particles makes it capable of working with advanced history-dependent soil constitutive models and; finally, the background mesh makes the application of the boundary conditions easier compare to other mesh-free methods. Although it can be argued that other mesh-free methods have similar features, the study aims to show that MPM is a very suitable framework for serving the purpose of the study.

The most crucial component for modeling sensitive clay slopes is the constitutive soil model, which represents the stress-strain behavior of the soil. The capability to reproduce realistic strain-softening characteristics in the material model is necessary for more accurate numerical analyses (Rødvand et al., 2022). Some strain-softening constitutive soil models for sensitive clays have also been developed to aid the purpose (Dey et al. 2015, Zhang et al. 2018). In recent studies, highly non-linear post-peak strain-softening of sensitive clays has inspired the implementation of an exponential strength degradation equation (Equation 1) to capture the post-peak soil behavior (Wang et al. 2022, Tran and Solowski 2019).

$$s_u = s_{ur} + (s_{up} - s_{ur})e^{-\eta \varepsilon_d^p} \qquad (1)$$

where ε_d^p is the deviatoric part of the plastic strain tensor, s_{up} and s_{ur} are the peak and remolded undrained shear strength, respectively, and η is a shape factor controlling the strength degradation rate. A similar constitutive model has been used in this study. The shape factor (η) is required to calibrate the exponential functional form of this softening law against experimental data. Large values of η correspond to greater strength decrease with plastic strain accumulation (i.e., more brittle nature).

Including strain-softening features in numerical methods can lead to strain localization issues. To address this, Rots et al. (1985) proposed a smeared crack approach as a regularization technique. This method assumes that the total work dissipated by a shear band is equivalent to the fracture energy dissipated in a discrete crack. By calibrating the parameter η through numerical shear tests, where the thickness of a shear band is approximately equal to the size of mesh elements, a specific relationship between shear stress and strain can be obtained. The goal is to ensure that the areas under the stress-strain curve, representing fracture energy, are equal for each element size, thus minimizing mesh dependency in the numerical solution.

This study focuses on the effects of changes in peak strength, remolded strength, and shape factor on the final retrogression and runout when a failure occurs in a sensitive clay slope. For this, stress distribution and the progression of failure in a simple, sensitive clay slope have been illustrated. Afterward, parametric studies were performed on the strain-softening parameters of sensitive clays, the peak shear strength, remolded shear strength, and shape factor. It then discusses how these factors control retrogressive failure and post-failure slope response.

2 BASIS OF MPM FRAMEWORK

In MPM, the continuum is discretized into a set of subdomains, and the mass of each sub-domain is carried by a certain number of material points (Figure 4).

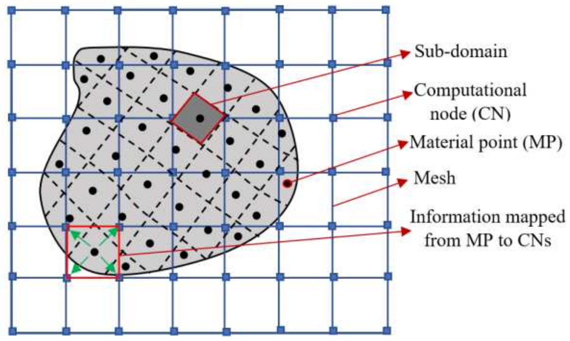

Figure 4. Spatial formulation of MPM framework

Material points (MPs) also carry properties like stresses, strains, velocities, accelerations, etc. The information is then mapped from MPs to the computational nodes of the background mesh. Governing equations are solved on the nodes, and updated information is mapped back to the MPs. The relationship between the MPs and the nodes at any domain point is defined with linear interpolation shape functions. The slope presented below is modeled using the two-phase single-point formulation executed in the MPM code Anura3D (www.anura3d.com). In the two-phase single-point approach (Ceccato et al. 2018), the saturated porous media is discretized by a single set of MPs which moves according to the solid velocity field. Each MP describes a representative volume element of fully saturated soil, carrying the information of both phases, solid and liquid. Displacements and velocities are updated based on calculated acceleration using an explicit Euler-Cromer scheme. A damping force is employed to avoid non-physical vibrations. This force is proportional to the out-of-balance force, and the proportion should be chosen wisely (very low for dynamic problems) to obtain an accurate solution.

3 DESCRIPTION OF THE NUMERICAL MODEL

A simple 5m high, 25m long single layered sensitive clay slope is taken, inclined at 45° to the horizontal from crest to toe (Figure 5). The slope rests on a firm base restricted for horizontal and vertical movement, whereas only horizontal movement is allowed at the left boundary. As the slope is expected to experience retrogressive failure, the length of the background mesh is extended up to 55m from the left slope boundary, and the height is 6m so that the soil particles have sufficient space for movement after failure. The computational mesh is discretized with three noded triangular elements with an average size of 0.3m. This size was determined through trial and error, considering larger and smaller sizes to achieve minimal mesh dependency while maintaining reasonable computational time. The analysis is performed in plane strain condition, and gravity loading is applied to generate the initial stress state of the slope. This non-physical stage involves instantaneously applying the full gravity load to the slope. To prevent any abrupt blasting effects of the sudden load on the material points, it is imposed that the material behaves elastically during this stage. Failure has been initiated by introducing the strain-softening behavior of sensitive clays in the subsequent calculation step after gravity loading.

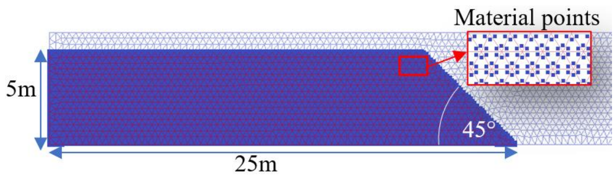

Figure 5. Slope geometry, meshing, and material points description of the numerical model

The undrained shear strength of sensitive clays can be as high as 100kPa or more. However, for different retrogressive landslide locations of eastern Canada, 7 out of 9 sites had an undrained shear strength from 20kPa-50kPa (Tavenas et al. 1983), and this parameter varied from 15-35kPa for 10 out of 14 previous landslide locations of Norwegian quick clays (Thakur and Degago 2012). The remolded shear strength for these sites was 0.2-2.1kPa for Canadian soils and 0.15-0.8kPa for Norwegian locations. Therefore, to demonstrate the process of retrogressive failure, peak, and remolded undrained shear strengths were taken to be 30kPa and 2kPa, respectively. And the post-peak degradation is exponential, as described in Equation 1. The rate of strength decrease depends on the shape factor η. For the taken strength values (30kPa and 2kPa), retrogressive failure doesn't occur in the simulated model for a shape factor <60. Therefore, the shape factor is assumed to be 70. The stress-strain curve adopted for the numerical model is illustrated in Figure 6. The elastic modulus is 5Mpa for soft sensitive clays, and the Poisson's ratio is 0.45 to replicate undrained conditions.

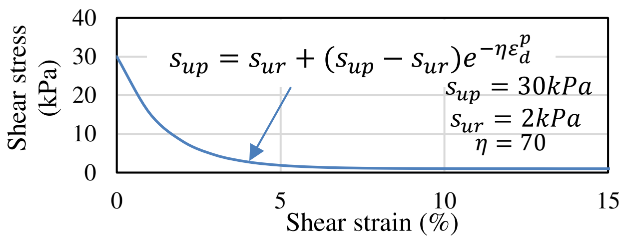

Figure 6. Strain-softening behavior was adopted for the demonstration of retrogressive failure.

The effect of post-failure retrogression and runout has been analyzed for parametric studies. The range for the soil parameters is primarily based on the soil properties of historical sensitive clay landslide locations (Tavenas et al. 1983, Thakur and Degago 2012). However, for the taken slope geometry of the simulated model, failure doesn't occur beyond an undrained shear strength of 30kPa. Additionally, for a fixed shape factor, there is a range for the shear strength values (both peak and remolded) below which retrogression doesn't stop (slope remains unstable) and beyond which retrogressive failure doesn't occur and vise-versa. Therefore, parametric studies have been performed considering all the factors mentioned above.

Table 1. Parametric studies

S_{up} (kPa)	S_{ur} (kPa)	η	S_t	L_R (m)	L_O (m)
30	1.0	65	30	>20	>35
30	1.3	65	23	16.2	33.5
30	1.8	65	17	15.8	31.0
30	2.5	65	12	13.5	27.9
30	3.2	65	9	10.8	24.5
19	2.8	45	7	17.5	26.8
22	2.8	45	8	15.5	25.2
25	2.8	45	9	16.1	25.6
28	2.8	45	10	10.7	24.6
20	2.0	65	10	18.2	32.6
25	2.5	65	10	13.6	28.1
30	3.0	65	10	14.5	25.3
25	3.0	20	8	4.0	23.8
25	3.0	40	8	11.2	25
25	3.0	60	8	13.3	26.5
25	3.0	80	8	17.8	26.2
25	3.0	90	8	18.4	28.0

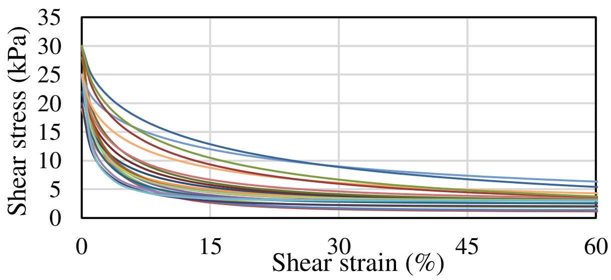

Figure 7. Strain-softening behavior adopted for the parametric studies.

Studies have been carried out, firstly, for a variation of remolded shear strength from 1.0 to 3.0 kPa, keeping the peak shear strength and shape factor constant; secondly, for a variation of peak shear strength from 15kPa to 30kPa keeping the other parameters unchanged, for a variation of both peak and remolded shear strength keeping the sensitivity constant and finally, changing the shape factor from 20 to 90 keeping other parameters the same. The material parameters for each trial are listed below, along with the final retrogression and runout in Table 1. Strain-softening curves adopted for the parametric studies are presented in Figure 7.

4 RESULTS

4.1 Mechanism of retrogressive failure

After the gravity loading in the first calculation step (Figure 8), the soil is stable with an undrained shear strength of 30kPa, and the strain starts to localize in a shear band as soon as strain softening is activated. When the failed soil mass starts to move forward as the first rotational slide happens, the drag of the liquified clay creates a shear band at a 45° angle to the horizontal. This process of strain localization can be found in Odenstad's (1951) hypothesis of the retrogressive spread failure mechanism, which later on was mathematically explained by Carson (1977). As failed soil mass continues progressing, consecutive 2nd, 3rd, and 4th slides occur. After the 4th slide, no new shear band is formed, and the failure stops after the failed soil mass from the 4th slide moves forward until the kinetic energy runs out. The final retrogression distance is (L_R)=15.8m, and the runout distance (L_O) is= 29.5m.

4.2 Effect of material parameters on post-failure movement

The peak and remolded shear strength both play a significant role in controlling the post-failure movement. However, it has been observed that runout in brittle soils has a significant impact and is primarily determined by remolded strength (Yerro et al. 2016). Zhang et al. 2018 illustrated that when the remolded shear strength approaches zero, both the final runout distance and retrogression distance become very large. Additionally, an increase in sensitivity leads to greater final runout and retrogression distances. Therefore, it is tough to assess the effect of varying peak or remolded shear strength on runout and retrogression because changing either of them and keeping the other constant changes the sensitivity of the soil, and sensitivity also affects the post-failure movement. Moreover, the overall effect of the shear strength parameters on the post-failure movement is highly influenced by the rate of strength decrease of the sensitive clay (Zhang et al.

2018, Wang et al. 2022), which makes it even more challenging.

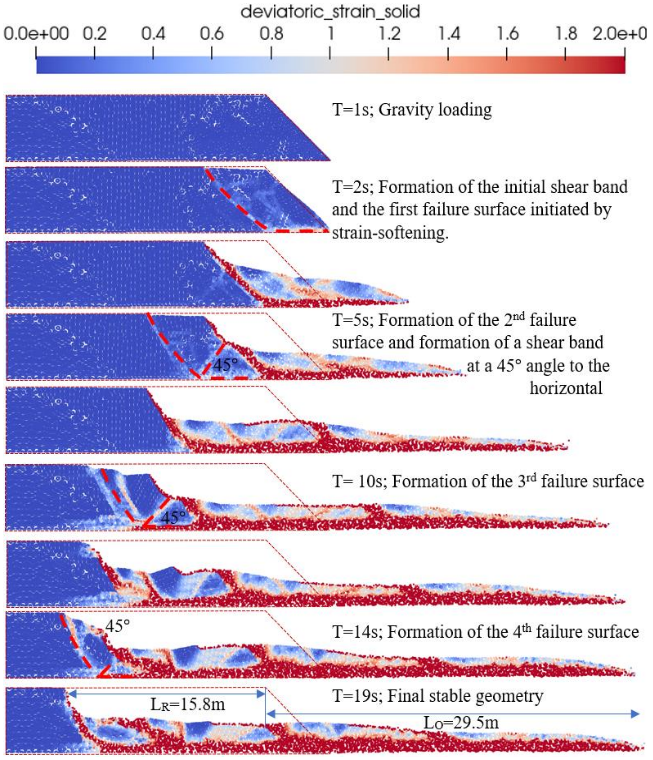

Figure 8. Mechanism of retrogressive failure

Increasing the remolded shear strength decreases the sensitivity, and as a result, the retrogression and runout distance substantially reduce (Figure 9). For an increase of remolded shear strength just by 0.9kPa, the retrogression distance reduces by 5.4m, and the runout reduces by 9m. If remolded shear strength keeps increasing, it reaches a specific value at which the failure stops at the first slide, and retrogression does not occur. The limiting value of remolded strength depends on the peak-shear strength and shape factor. For example, for 30kPa peak strength with a shape factor of 65, retrogressive failure doesn't occur beyond a remolded strength of 3.3kPa. Therefore, for a particular geometry and stress-strain profile, there is a unique value of remolded shear strength above which the failure would no longer be retrogressive.

The effect of varying peak-shear strength on the post-failure movement is not as straightforward as for remolded shear strength because sensitivity also increases with increasing peak shear strength. It is observed that retrogression and runout decrease with increasing peak strength (Wang et al., 2022). At the same time, retrogression increases with increased sensitivity (Zhang et al. 2018). These two factors are counterproductive. Therefore, to assess the effect of varying peak strength on the final runout, the change in sensitivity is kept as low as possible. An increase in peak strength decreases the retrogression and runout in most cases but doesn't have as significant an impact as the remolded shear strength. For a peak strength variation of 9kPa and sensitivity by 3, the retrogression reduces by 6.8m, and the runout reduces by only 2m. This effect is reflected in the MPM results presented in Figure 10. With the increase of peak-shear strength and simultaneous increase of sensitivity, there is a minimal change in post-failure runout. It could be because increased peak strength counters the effect of increased sensitivity.

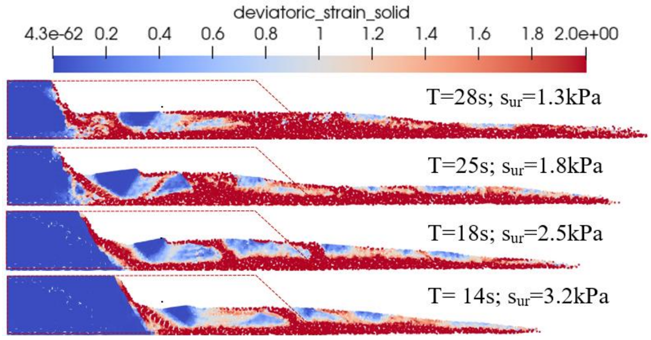

Figure 9. Effect of remolded shear strength on post-failure movement

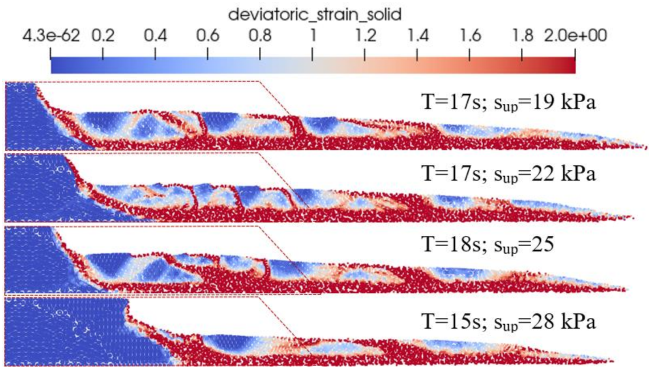

Figure 10. Effect of peak shear strength on post-failure movement

Another study has assessed the impact of the varying peak and remolded strength when the sensitivity is kept constant. It is observed that an increase in both peak and remolded shear strength decreases the post-failure movement (Figure 11).

The shape factor (η) controls the rate of strength reduction. It has been observed that, for a fixed pair of peak and remolded strength values, an increase in shape factor significantly increases the retrogression distance (the number of successive slides). Runout distance also increases with an increasing shape factor.

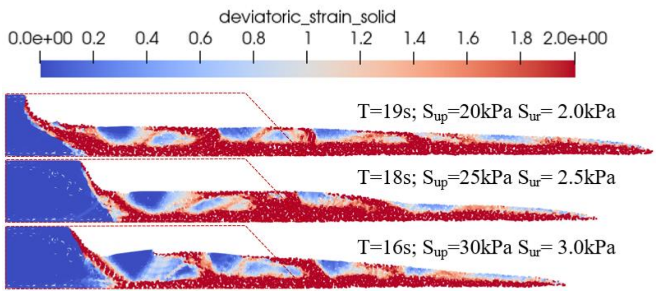

Figure 11. Effect of changing peak and remolded shear strength on post-failure movement with constant sensitivity

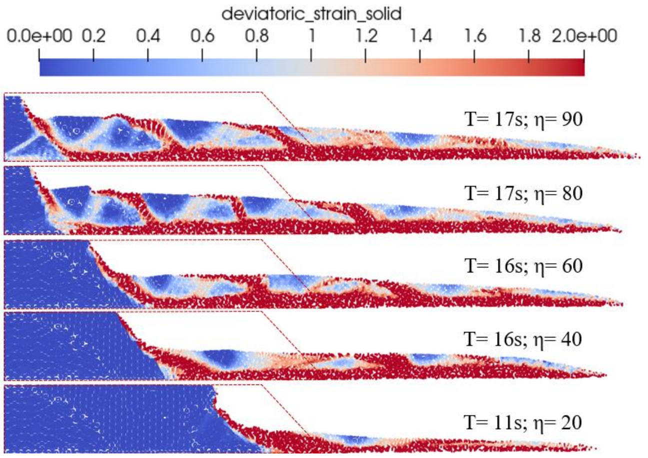

Figure 12. Effect of the shape factor on post-failure movement with constant sensitivity

5 CONCLUSION

This study has thoroughly assessed the effect of strain softening for retrogressive failure and associated post-failure movements. It can be concluded that,

- Strain-softening causes strain localization forming narrow shear bands, which create subsequent failure surfaces, eventually leading to retrogressive failure
- The occurrence of retrogressive failure significantly depends on a low value of remolded shear strength. The remolded shear strength should be low enough to cause strain localization within a narrow shear band.
- For a fixed sensitivity, higher values of peak and remolded shear strength results in lower post-failure movement.
- For a fixed value of peak and remolded shear strength, the rate of strength reduction factor/ shape factor has a marginal value; less than this value will not cause retrogressive failure
- The effect of sensitivity and peak shear strength on the occurrence of retrogressive failure vastly depends on the remolded shear strength and the shape factor. A set of particular peak shear strengths and sensitivity may not cause a retrogressive failure if the shape factor is too low or the remolded strength is too high.

6 REFERENCES

Carson, M.A., 1977. On the retrogression of landslides in sensitive muddy sediments. *Canadian Geotechnical Journal* **14**, 582–602.

Ceccato, F., Yerro, A., Martinelli, M.2018. Modelling soil-water interaction with the material point method. Evaluation of Single-Point and Double-Point Formulations. NUMGE IX. Volume 1, CRC Press; 2018: 351.

Dey, R., Hawlader, B., Phillips, R., Soga, K., 2015. Large deformation finite-element modelling of progressive failure leading to spread in sensitive clay slopes. *Geotechnique* **65**, 657–668.

Lefebvre, G. 1996. Soft Sensitive Clays. *Landslides: investigation and mitigation, Special report 247, Transportation Research Board*. National Academy Press, Washington, DC, pp 607–619. Washington, DC.

Locat A., Leroueil S., Bernander S., Demers D., Jostad H.P., and Ouehb L. 2011. Progressive failures in eastern Canadian and Scandinavian sensitive clays. *Canadian Geotechnical Journal*, **48**(11): 1696–1712

Locat, A., Jostad, H.P., Leroueil, S., 2013. Numerical modeling of progressive failure and its implications for spreads in sensitive clays. *Canadian Geotechnical Journal* **50**, 961–978.

Odenstad, S., 1951. The landslide in Skoptrop on the Lidan river, in: *Royal Swedish Geotechnical Institute Proceedings No. 4*.

Rødvand, L.A., Jostad, H.P., Grimstad, G., Andresen, L., 2022. Strain localisation in sensitive clays: can rate dependency provide mesh independent results? *Computers and Geotechnics* **145.**

Rots, J., Nauta, P., Kuster, G., Blaauwendraad, J. 1985. Smeared crack approach and fracture localization in concrete. *HERON 30*, **1**, 3–48.

Rosenqvist, I.T. 1953. Considerations on the sensitivity of norwegian quick-clays. *Géotechnique* **3**, 195–200.

Skempton, A.W., Northey, R.D. 1952. The sensitivity of clays. *Géotechnique* **3**, 30–52.

Sulsky, D., Chen, Z., Schreyer, H.L. 1994. A particle method for history-dependent materials. *Computer Methods in Applied Mechanics and Engineering* **118**, 179–96.

Tavenas, F., Flon, P., Leroueil, S., Lebuis, J., 1983. Remolding energy and risk of retrogression in sensitive clays, in: *Proceedings of the Symposium on Slopes on Soft Clays*.

Thakur, V., Degago, S.A., 2012. Quickness of sensitive clays. *Geotechnique Letters* **2**, 87–95.

Tran, Q.A., Sołowski, W., 2019. Generalized Interpolation-Material Point Method modelling of large deformation problems including strain-rate effects – Application to-penetration and progressive failure problems. *Computers and geotechniques* **106**, 249–265.

Wang, C., Hawlader, B., Perret, D., Soga, K. 2022. Effects of geometry and soil properties on type and retrogression of landslides in sensitive clays. Géotechnique **72**, 322-336.

Wang, B., Vardon, P.J., Hicks, M.A. 2016. Investigation of retrogressive and progressive slope failure mechanisms using the material point method. *Computers and Geotechnics* **78**, 88–98.

Yerro, A., Alonso, E.E., Pinyol, N.M. 2016. Runout of landslides in brittle soils. *Computers and Geotechnics* **80**, 427-439.

Zhang, X., Sloan, S.W., Oñate, E., 2018. Dynamic modelling of retrogressive landslides with emphasis on the role of clay sensitivity. *International Journal for Numerical and Analytical Methods in Geomechanics* **42**, 1806–1822.